Borehole Ground Penetrating Radar attribute analysis for urban engineering

Wenke Zhao [a,b,*], Ming Huang [c], Baojie Wu [d], Xucheng Hong [c], Emanuele Forte [e], Michele Pipan [e]

[a] Key Laboratory of Geoscience Big Data and Deep Resource of Zhejiang Province, School of Earth Sciences, Zhejiang University, Hangzhou 310058, PR China
[b] Key Laboratory of Intelligent Detection and Equipment for Underground Space of Beijing-Tianjin-Hebei Urban Agglomeration, Ministry of Natural Resources, Shijiazhuang 050031, PR China
[c] Zhejiang Engineering Geophysical Prospecting and Design Institute Co., LTD, Hangzhou 310000, PR China
[d] Zhejiang Academy of Building Research & Design Co., LTD, Hangzhou 310012, PR China
[e] Department of Mathematics and Geosciences, University of Trieste, Trieste 34127, Italy

ARTICLE INFO

Keywords:
Borehole Ground Penetrating Radar
Attribute Analysis
Urban Geophysics
Subway Construction

ABSTRACT

A precise and detailed knowledge and characterization of the subsurface is crucial for urban engineering planning and implementation. Drillings/boreholes are most widely used to provide the spatial distribution of blocks and boulders, but it is difficult to determine with high spatial-resolution location and distribution of the blocks and boulders in the soil stratum. We evaluate the applicability and the effectiveness of borehole Ground Penetrating Radar (GPR) for urban engineering purpose and we test attribute analysis to help the subway construction in the city center of Hangzhou, China. A multi-attribute approach exploiting amplitude-based and textural attributes is used. The results demonstrate that attribute analysis can visualize and quantitatively characterize borehole GPR features in an automatic and objective manner, maximizing the information for urban engineering. The integrated results from drillings and borehole GPR can provide an effective distribution of localized heterogeneities (such as blocks/boulders, sand/gravel lenses, cavities) in the potential target area.

1. Introduction

With the rapid social and economic development, underground constructions for civil infrastructure are becoming increasingly important in urban areas (e.g. Metje et al., 2007; Ronczka et al., 2018). In this general context, a precise and detailed knowledge and characterization of the subsurface is crucial for urban engineering planning and implementation. Direct investigation methods like trenches or boreholes are widely used and effective, but they cannot provide a continuous high-resolution spatial information, as the number of boreholes is often limited to save the cost of the investigations and to avoid possible risks of damaging buried infrastructures. Therefore, cost-effective and non-invasive geophysical methods are becoming more and more important in urban settings (e.g. Dobecki, 2010; Diallo et al., 2019), and this field of study is generally referred as 'urban geophysics' (e.g. Miller, 2013). In contrast to conventional geophysical exploration, the undertaking of urban geophysics is often challenging due to such factors as ambient cultural noise, a higher exploration resolution requirement, logistical constraints and illegible shallow targets buried within the heterogeneous layers with miscellaneous man-made objects (Liu and Chan, 2007).

Ground Penetrating Radar (GPR) is an extremely high-resolution geophysical technique to image and characterize subsurface urban engineering targets on the base of changes in the electro-magnetic properties of the materials, and GPR has been widely used for the identification of probable subsurface voids (e.g. Luo and Lai, 2020), the pavement detection / road quality evaluation (e.g. Grote et al., 2005; Wang et al., 2022), the characterization of karst hazards / active sinkholes in urban areas (e.g. Carbonel et al., 2014; Rodriguez et al., 2014), the assessment of fracturing and mechanical damage in tunnel ahead prospecting (e.g. Caselle et al., 2020), and the testing of structural integrity and long-term performance of the tunnel lining / dikes and dams (e.g. Di Prinzio et al., 2010; Kravitz et al., 2019), among the others. Meanwhile, the effectiveness of GPR is seriously constrained by complicated surface conditions, limited penetration depth and electric interference and noises.

* Corresponding author at: Key Laboratory of Geoscience Big Data and Deep Resource of Zhejiang Province, School of Earth Sciences, Zhejiang University, Hangzhou 310058, PR China.
E-mail address: zhaowenke@zju.edu.cn (W. Zhao).

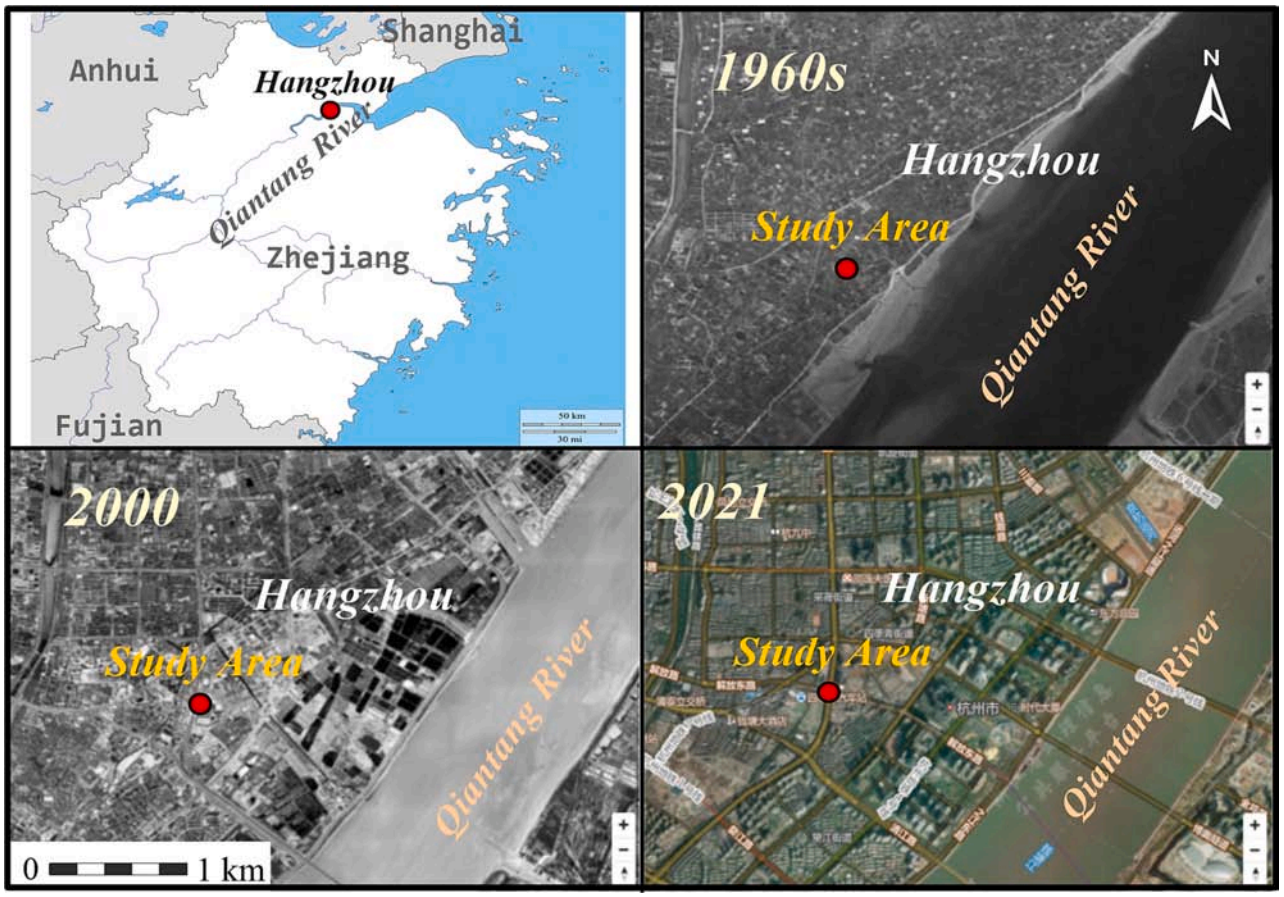

Fig. 1. Location map of the study area, and the remote sensing images in different historical periods.

Within this context, borehole GPR can be used to acquire high SNR (Signal to Noise Ratio) data, as the transmitting and receiving antennas are closer to the potential engineering targets, resulting in more precise target responses, and to overcome, at least partially, the penetration depth limits (e.g. Wänstedt et al., 2000; Kapustin et al., 2009). Borehole GPR can be operated in a single borehole, between two boreholes (i.e. cross-hole GPR), and from a borehole to the surface / a tunnel, i.e. Vertical Radar Profiling - VRP (Slob et al., 2010; Tronicke and Hamann, 2014). In the single borehole measurement, the transmitting and receiving antennas with a fixed distance apart are moved into the borehole at regular intervals (Serzu et al., 2004). Although the surrounding conditions of the antennas are very different from surface GPR surveys, the principle of the single borehole measurement is similar to that of surface GPR technique, and thus can share similar processing and interpretation techniques (Spillmann et al., 2007). Of course, it cannot be ignored that the transmitting and receiving antennas of borehole GPR are omnidirectional and the received radar waves are therefore potentially coming from any direction in the space (Li et al., 2021). On the contrary, cross-hole GPR and VRP often exploit tomographic approaches with the aim to obtain either the EM velocity field from traveltimes, or the attenuation values from amplitudes (or both of them) (e.g. Tronicke and Hamann, 2014).

In order to detect possible underground obstacles and to help the subway planning and construction, we designed and completed a series of borehole GPR surveys in the city center of Hangzhou, China. Borehole GPR measurements can cover the lack of information between adjacent boreholes and attribute analysis can further facilitate the identification and characterization of subsurface targets improving the overall quality and effectiveness of GPR interpretation for different application fields (e.g. Forte et al., 2012; Zhao et al., 2013, 2016a, 2016b, 2018; Forte et al., 2021; Allroggen et al., 2022). We tested the applicability and the performances of borehole GPR attribute analysis in urban engineering with the aim to better characterize the buried targets and evaluate the distribution of localized heterogeneities in the subsoil.

2. The study area

The construction of the subway has been significantly increased in Hangzhou, China, in recent years, with the crucial objective to reduce the traffic congestion and to meet the increasing travel requirements of residents. The study area is located at the Road Qiutao, in the center of Hangzhou (Fig. 1), where the Sijiqing Station of the subway will be built. Previous geotechnical investigations found that there is an ancient river embankment in the area, which was built with block stones or strip stones along the ancient Qiantang River during the Ming and Qing Dynasties (i.e. from XIV to XIX centuries). The region of Qiantang River is the most directly and violently affected by the sea tide in the southeast coast of China. The river embankment (usually called *seawall* in this region), an important barrier for tide control in the estuary area of Qiantang River, is one of the grandest and technologically advanced

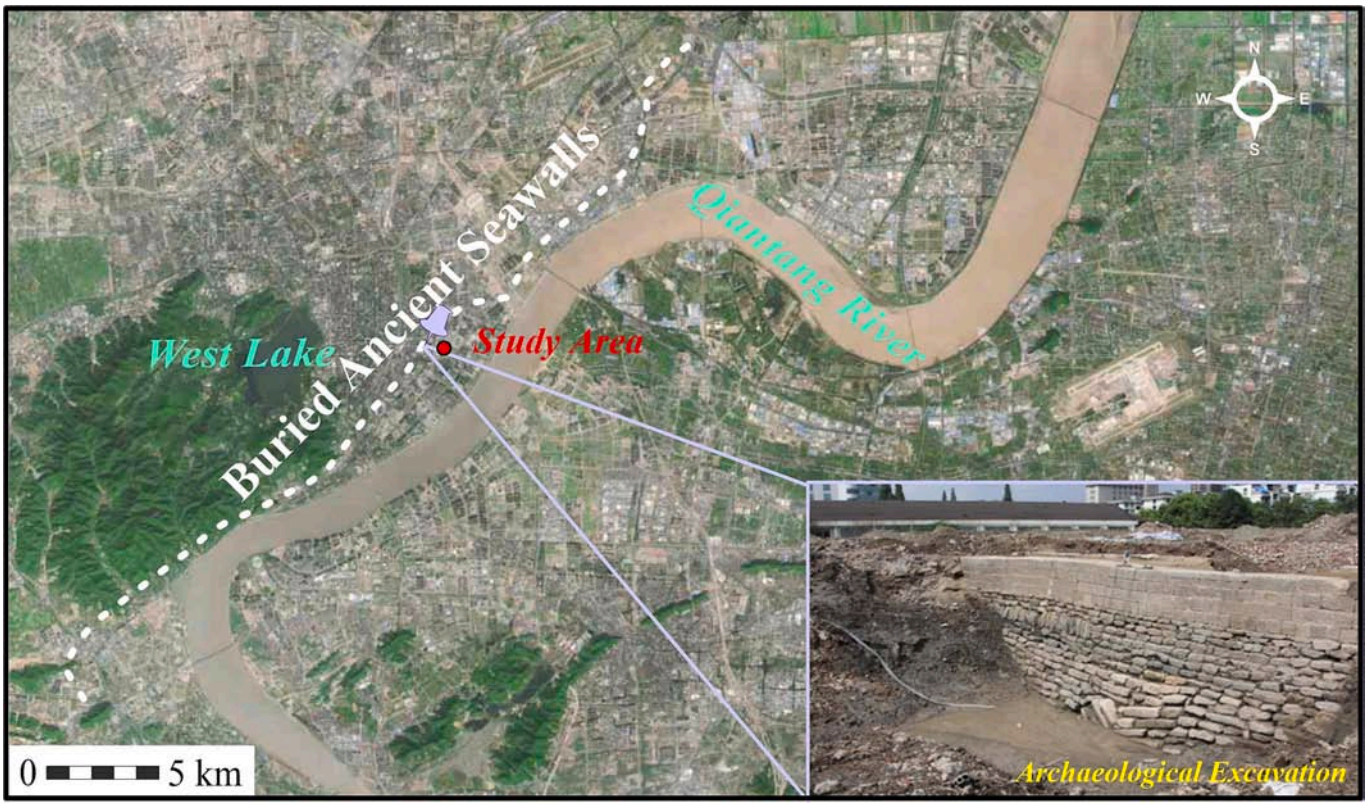

Fig. 2. Present map with highlighted the location of the ancient seawalls in *Hangzhou section* and a photograph of an archaeological excavation of the seawall close to the study area (adapted from Jin, 2018).

ancient artificial tide retaining dikes in the whole China (e.g. Xu, 2004; Jin, 2018).

The first round of large-scale construction was carried out in the Tang and Song Dynasties (VI-X centuries). The construction of seawalls was gradually greatly developed since Qian Liu established the Kingdom of Wuyue in the X century, when Hangzhou became the capital of the local separatist regime. The second comprehensive expansion of the seawalls was carried out with block stones or strip stones during the Ming and Qing Dynasties (Wang et al., 2018), and the location of '*Hangzhou Section*' (Fig. 2) was found and excavated by archaeologists in recent years (Jin, 2018). Besides, the building materials are mainly tuff and quartz sandstone. Due to the strong tidal current at the Qiantang River estuary, the location of the river has changed frequently. Although many ancient seawalls are relatively intact and still in use today, with the change of the streamway, many seawalls have retreated inland and no longer face the river, and even been destroyed or buried.

Nowadays there is a certain distance between the location of the study area and the actual Qiantang River, while we can also see the former Qiantang River was much wider, as apparent for instance in the remote sensing image of 1960s (Fig. 1), as well as the former boundary of the river was closer to the study area. It is planned to build an underground passage with pipe jacking at the Entrance and Exit C and D of Sijiqing Station to meet the street crossing function. It is estimated that the construction length of the pipe jacking is 67 m and the width is 6 m. In order to ensure the construction safety and to plan the subsequent implementation of infrastructures, it is necessary to detect whether there are isolated blocks and how is their distribution in the 8–13 m depth range.

3. Methods

Several drillings and borehole GPR measurements were carried out during Oct-Nov, 2021 in the study area. The arrangement of the data acquisition is shown in Fig. 3, while Table 1 provides the depths for all the drillings. A Malå Geoscience GPR system equipped with 100 MHz central-frequency borehole antennas was used to perform single borehole data acquisition within all the drilled boreholes, with a constant 0.025 m trace distance, in the selected test site. Due to the total length of the antenna equal to 4.566 m, we cannot get valid measurements at a depth shallower than 2.283 m (i.e. the midpoint of the selected antenna). The basic processing sequence was similar to surface GPR data and included: data editing, geometry header definition, DC removal, amplitude analysis, spectral analysis, band-pass filtering, background removal, and amplitude recovery.

As previously mentioned, attribute analysis can facilitate the identification and characterization of subsurface and improve the efficiency and effectiveness of data interpretation, so we calculated amplitude-related and textural attributes to highlight the potential targets. Besides, composite displays, combining information from more than one attribute into a single display, were exploited to allow an improved visual interpretation.

3.1. Amplitude-related attributes

Amplitude-related attributes belong to the most common attribute category in seismic/GPR applications, as they can help highlighting the main lateral changes and detecting subsurface materials variations. We

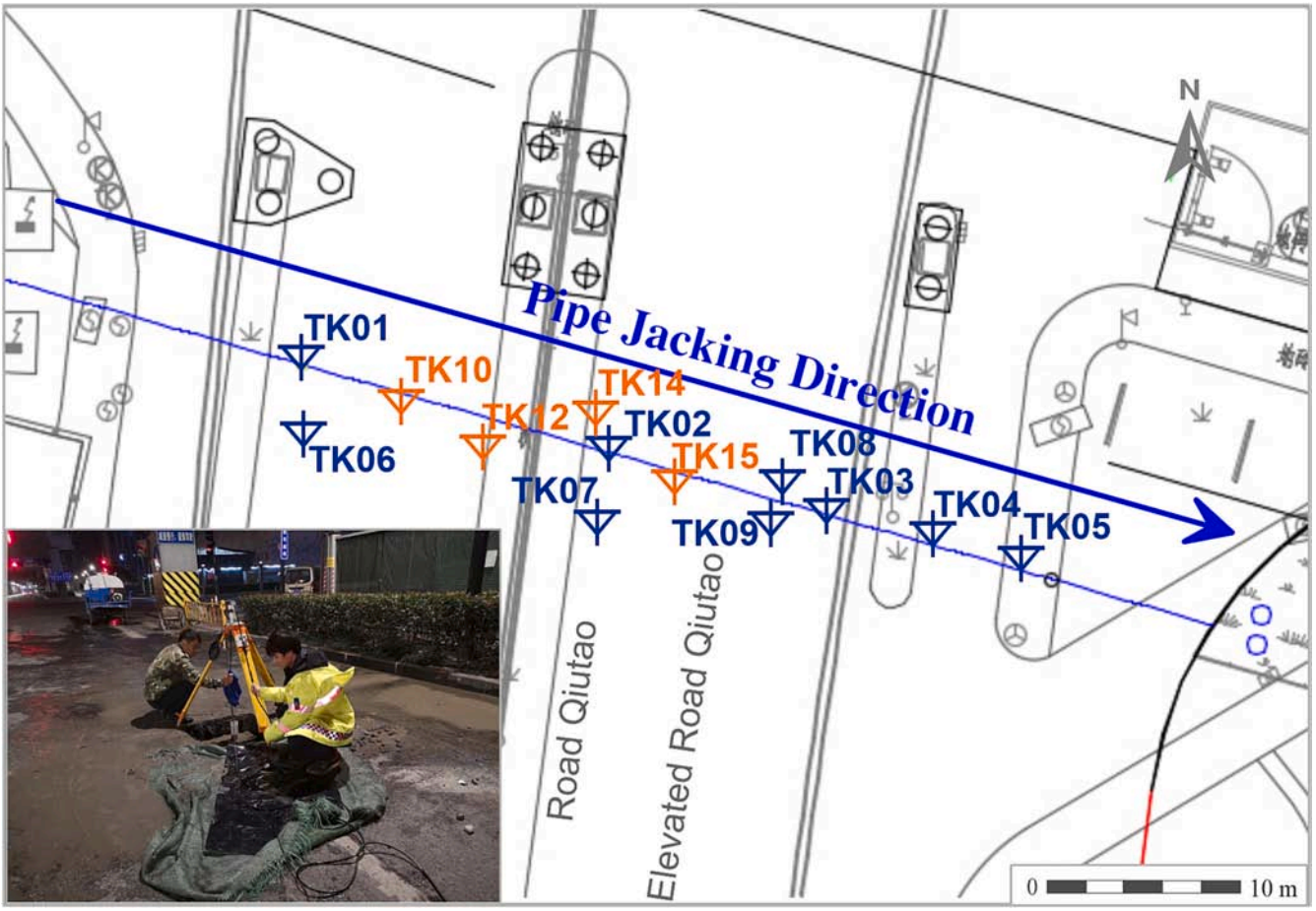

Fig. 3. Layout of borehole GPR acquisition and a photograph showing data acquisition operations. The different colors of the drilling symbols mean different data acquisition times (Orange ones were carried out after the blue ones, for the purpose of encrypting measurements). (For interpretation of the references to colour in this figure legend, the reader is referred to the web version of this article.)

Table 1
Different depths for all the drillings.

Drilling No.	Total depth (m)	Drilling No.	Total depth (m)
TK01	15.0	TK08	17.0
TK02	15.0	TK09	17.0
TK03	15.0	TK10	18.0
TK04	16.0	TK12	16.0
TK05	17.0	TK14	18.0
TK06	17.0	TK15	16.0
TK07	17.0		

calculated Amplitude First Derivative (i.e. Amplitude 1st Derivative), to enhance identifiable reflections of borehole GPR data (further details in Zhao et al., 2018).

3.2. Textural attributes

Textural attributes use the repeating patterns of local variations in image intensity, and a gray-level co-occurrence matrix (GLCM) algorithm (Haralick et al., 1973). They are commonly used to compute second-order statistical measures of textural characteristics such as energy, homogeneity, cluster, and entropy. We calculated the Contrast attribute to highlight the local variation of the borehole GPR data in the study (further details in Zhao et al., 2016b).

3.3. Multi-attribute display

Single attributes can partly and separately display details related to different physical and geometrical properties of the subsurface, while the multi-attributes display approach can improve the overall subsurface imaging by combining information from more than one attribute into a single display (Zhao et al., 2016a, 2018). In the present case, overlaying is used to merge Amplitude 1st Derivative and Contrast, being the first attribute plotted in variable area format and overlaid on the second attribute lying on the background.

4. Results

A total of 13 drillings were carried out in the study, among which blocks were widely distributed in the miscellaneous fill of shallow subsurface. TK03 and TK04 revealed larger blocks in the depth range of 10–11.5 m, while a small number of blocks was found locally in the other drillings. Besides, four soil layers such as the miscellaneous fill, the plain fill, the sandy silt, and the silt can be discerned from the surface to the deep part. A correlation of stratigraphic columns of some drillings along the direction of pipe jacking (drillings TK01, TK02, TK03, TK04, TK05, TK09, and TK10) is provided in Fig. 4. We defined the interfaces

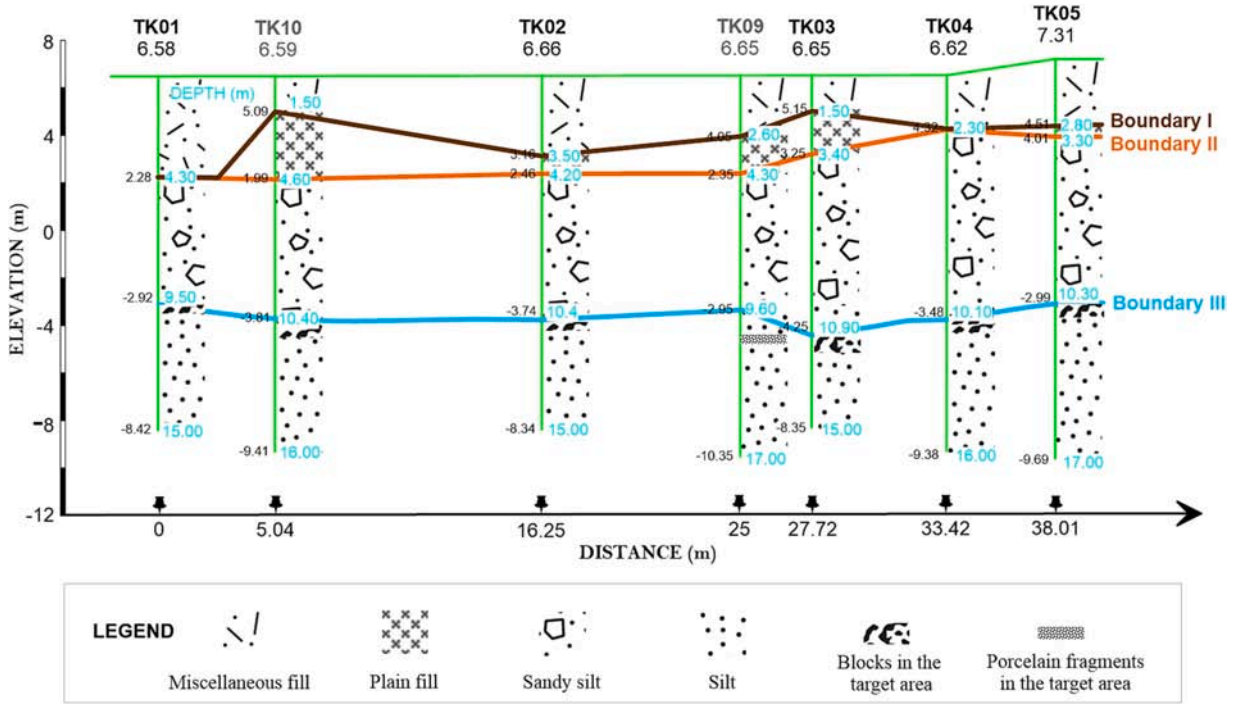

Fig. 4. Schematic stratigraphy of drillings TK01, TK02, TK03, TK04, TK05, TK09, and TK10 along the direction of pipe jacking. Boundary I, II, III mark different soil and sedimentary layers.

between the miscellaneous fill, the plain fill, the sandy silt, and the silt as Boundary I, II, III respectively. From Fig. 4, it is apparent that abrupt lateral variations occur even between very close drillings like TK1 and TK10 or TK9 and TK3. Moreover, the drilling samples of TK04, TK05 and TK09 are selected as exemplary for all the drillings because they summarize all the typical characteristics of the study area (Fig. 5).

Fig. 6 provides Amp 1st derivative, Texture-Contrast and multi-attribute displays based on borehole GPR measurement in drillings TK04, TK05 and TK09. 100 MHz central-frequency borehole antennas used in the study allowed a penetration range of about 3 m radial depth, considering an empirical and constant EM velocity value equal to 0.07 m/ns. We can see that amplitude-related attribute can highlight the overall reflectivity, making the major changes more apparent, while the Contrast textural attribute emphasize the differences between reflection patterns. Besides, composite displays (i.e. the overlay display) by virtue of data fusion can get higher- recognition results. Since the antennas are omnidirectional, the results obtained by the borehole GPR do not refer directly and only to the borehole stratigraphy but rather summarize the information in the vicinity (approximately in a circle having a 3 m long ray) of each borehole.

We identified moderately weathered tuff blocks in the 10.1–10.6 m range from drilling samples. Based on this calibration, the analysis of the borehole GPR data attributes indicates that blocks are significantly distributed around the boreholes in this depth range (as indicated by the white rectangle). Furthermore, there is also another anomaly in the borehole GPR attributes associated with blocks in the range 7.8–9.0 m (as indicated by the orange rectangle). Compared with the samples of TK04, the size of the blocks in the range 10.3–10.9 m for TK05 is much smaller. In this borehole the GPR results indicate a diffuse anomaly in the range 9.8–13.0 (see purple rectangle) and there is also another strong anomaly associated with blocks in the range 7.0–8.5 m (purple ellipse). In addition, ancient porcelain fragments in the range 11.0–11.2 m are present in the samples from TK09. Similarly, a strong anomalous attribute associated with block / man-made objects can be found in the range of 9.8–11.8 m (red rectangle) from the borehole GPR results. It is also worth noting that there is another strong anomaly in the attributes in the shallower subsurface (white ellipse), although this falls outside the scope of our potential interests.

After correlating the multi-attribute displays with the stratigraphic columns of drillings (Fig. 7), we can find that different reflection patterns can be recognized around the Boundary III. In fact, the relative larger local variations between the Boundary II and III, can be associated with the layer of sandy silt; while the smaller local variations below the Boundary III can be associated with the silt layer. Moreover, a mixed layer (between the white line and the Boundary III) is associated with the presence of large blocks/artificial objects embedded into the silt soil. Furthermore, by virtue of borehole GPR attribute analysis, it is easier to get accurate, well-correlated and convincing soil stratigraphic divisions.

5. Discussion and conclusions

We can see that the position of the study area is inside the ancient seawall from Fig. 2. The soil made of sandy silt and silt belongs to mixed alluvial and marine sediments in this region, so the presence of blocks can be considered not natural, but rather related to human activities through the history. This is further testified by the presence of ancient porcelain fragments within the soil stratum (see Fig. 4). In particular, the blocks from the drillings are made by tuff, which is consistent with the building materials of ancient seawalls. According to its depth and nature, it can be considered that the blocks within the target area are related to residuals of the ancient seawalls formed by river tides that continuously scoured the seawalls.

The identification of blocks in the subsurface soil has been challenging due to their random distribution, different shapes and

Fig. 5. Drilling samples of TK04, TK05 and TK09. Blocks and ancient porcelain fragments can be found in the target area (i.e. 8–13 m depth range).

dimensions, irregular development, and indefinite burial depth, which has also brought great difficulties for urban engineering projects and infrastructures implementation. Drillings/boreholes are most widely used to provide the spatial distribution of the blocks and to ensure a smooth progress of subway construction. Compared with the usual drilling spacing equal at maximum to 25 m in the exploration stage for subway projects, it is impossible to determine the high-resolution spatial location and distribution of blocks in the subsoil even if densifying the drillings, which is in any case unrealistic, due to constraints related to the cost and logistical conditions. Single boreholes certainly provide precise stratigraphic information but the correlation of the results is often challenging.

The results of our study demonstrate that borehole GPR is a useful tool for urban geophysics, to get accurate and convincing subsurface stratigraphic correlations and material characterization, especially if it is combined with stratigraphic and other ancillary data like archaeological excavations and morphological information, as in the present case. Attribute analysis can facilitate the identification and characterization of subsurface improving the overall quality of interpretation. Composite displays of different attributes by virtue of data fusion are helpful to better recognize distinct reflection patterns and distinct signal signatures, which are in turn related to physical property, geometry, texture, and peculiar characteristics of potential urban engineering targets.

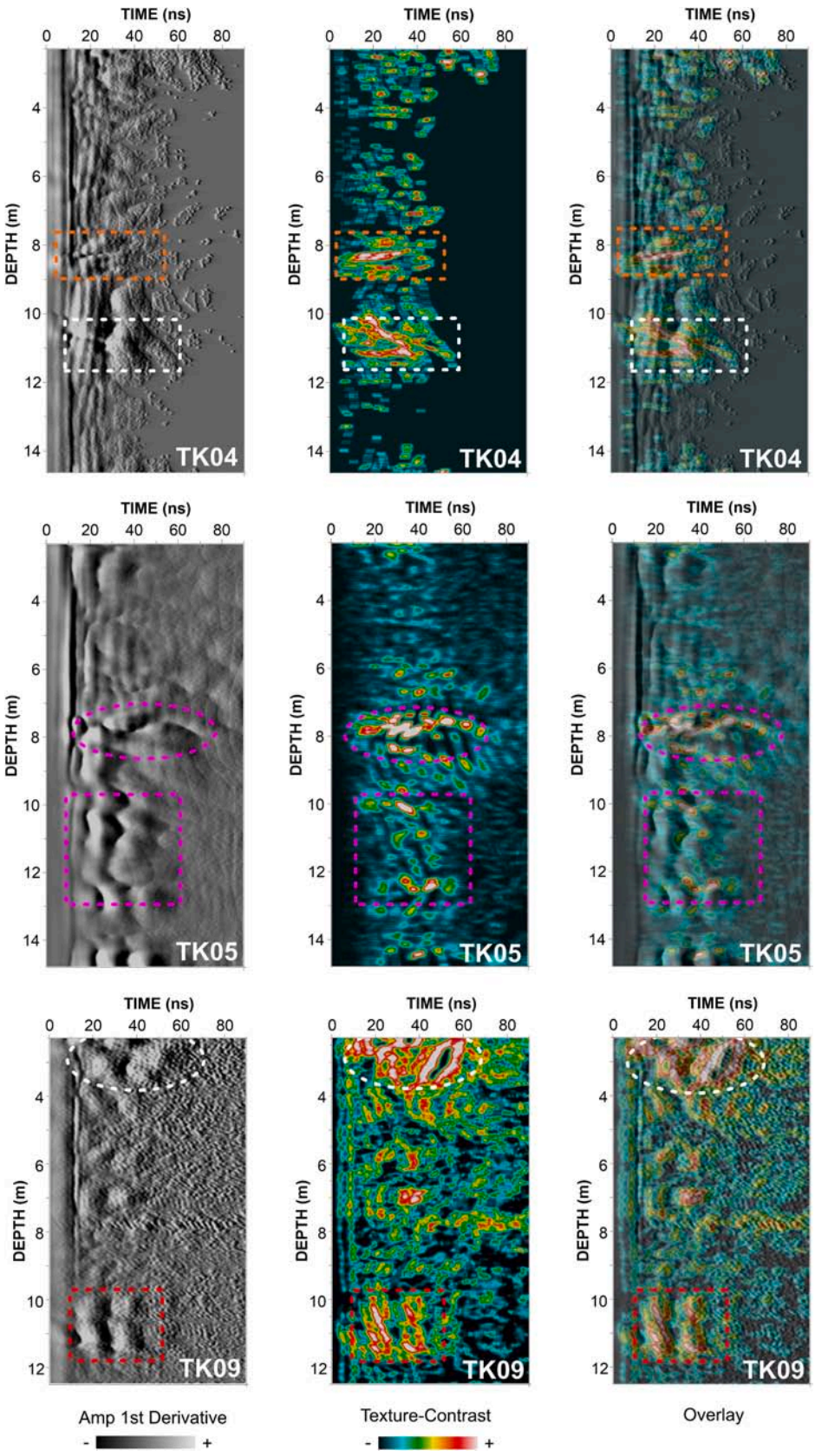

Fig. 6. Amp 1st derivative, Texture-Contrast and multi-attribute displays (from left to right) based on borehole GPR measurement in drillings TK04, TK05 and TK09. Different reflectivity and reflection patterns can be recognized; the most significant features are indicated with different colored guidelines.

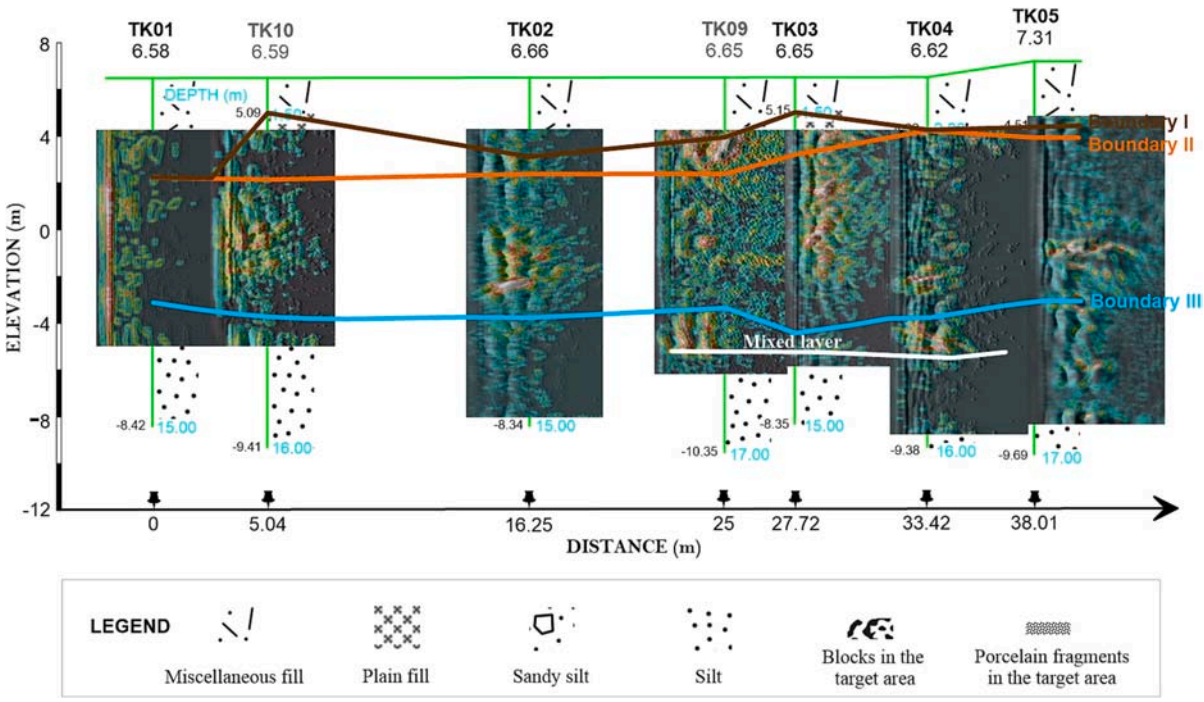

Fig. 7. The multi-attribute displays are correlated with the stratigraphic columns of drillings TK01, TK02, TK03, TK04, TK05, TK09, and TK10.

CRediT authorship contribution statement

Wenke Zhao: Writing – original draft. **Ming Huang:** Data curation. **Baojie Wu:** Resources. **Xucheng Hong:** Data curation. **Emanuele Forte:** Methodology. **Michele Pipan:** Methodology.

Declaration of Competing Interest

The authors declare that they have no known competing financial interests or personal relationships that could have appeared to influence the work reported in this paper.

Data availability

Data will be made available on request.

Acknowledgments

This research was supported by Key Laboratory of Intelligent Detection and Equipment for Underground Space of Beijing-Tianjin-Hebei Urban Agglomeration, Ministry of Natural Resources of China under Grant No. ZB2023002, and Zhejiang Provincial Natural Science Foundation of China under Grant No. LTGS23D040001. The authors thank dGB Earth Sciences for providing OpendTect open source seismic data analysis software, and two anonymous reviewers for providing thoughtful and useful suggestions.

References

Allroggen, N., Heincke, B.H., Koyan, P., Wheeler, W., Rønning, J.S., 2022. 3D GPR attribute classification: a case study from a paleokarst breccia pipe in the Billefjorden area on Spitsbergen, Svalbard. Geophysics. 87 (4), 1–52.

Carbonel, D., Rodríguez, V., Gutiérrez, F., et al., 2014. Evaluation of trenching, ground penetrating radar (GPR) and electrical resistivity tomography (ERT) for sinkhole characterization. Earth Surf. Process. Landf. 39 (2), 214–227.

Caselle, C., Bonetto, S., Comina, C., Stocco, S., 2020. GPR surveys for the prevention of karst risk in underground gypsum quarries. Tunn. Undergr. Space Technol. 95, 103137.

Di Prinzio, M., Bittelli, M., Castellarin, A., Pisa, P.R., 2010. Application of GPR to the monitoring of river embankments. J. Appl. Geophys. 71 (2–3), 53–61.

Diallo, M.C., Cheng, L.Z., Rosa, E., Gunther, C., Chouteau, M., 2019. Integrated GPR and ERT data interpretation for bedrock identification at Cléricy, Québec, Canada. Eng. Geol. 248, 230–241.

Dobecki, T.L., 2010. Sinkholes and pitfalls in urban geophysics. Lead. Edge 29 (8), 944–951.

Forte, E., Pipan, M., Casabianca, D., Di Cuia, R., Riva, A., 2012. Imaging and characterization of a carbonate hydrocarbon reservoir analogue using GPR attributes. J. Appl. Geophys. 81, 76–87.

Forte, E., Mocnik, A., Basso, P., Casagrande, G., Martinucci, D., Pillon, S., Possamai, M., Zambrini, R., 2021. Optimised extraction of archaeological features from full 3-D GPR data. Appl. Sci. 11, 8517.

Grote, K., Hubbard, S., Harvey, J., Rubin, Y., 2005. Evaluation of infiltration in layered pavements using surface GPR reflection techniques. J. Appl. Geophys. 57 (2), 129–153.

Haralick, R.M., Shanmugam, K., Dinstein, I.H., 1973. Textural features for image classification. IEEE Trans. Syst. Man Cybern. 6, 610–621.

Jin, Y., 2018. The Researches on the Current Situation and Chronicles Changes of Qiantang River Hangzhou Section. Zhejiang University (in Chinese).

Kapustin, V.V., Semeikin, N.P., Monakhov, V.V., 2009. Application of borehole ground penetrating radar for surveying underground engineering structures. First Break 27 (3), 87–90.

Kravitz, B., Mooney, M., Karlovsek, J., Danielson, I., Hedayat, A., 2019. Void detection in two-component annulus grout behind a pre-cast segmental tunnel liner using Ground Penetrating Radar. Tunn. Undergr. Space Technol. 83, 381–392.

Li, L., Wang, R., Peng, T., Hao, J., Zhou, Z., Han, Z., 2021. Identification of geo-bodies in borehole radar image based on Curvelet transform. J. Appl. Geophys. 189, 104325.

Liu, L., Chan, L.S., 2007. Sustainable urban development and geophysics. J. Geophys. Eng. 4 (3), 243–244.

Luo, T.X., Lai, W.W., 2020. GPR pattern recognition of shallow subsurface air voids. Tunn. Undergr. Space Technol. 99, 103355.

Metje N, Atkins PR, Brennan MJ, Chapman DN, Lim HM, Machell J, Muggleton JM, Pennock S, Ratcliffe J, Redfern M, Rogers CD. Mapping the Underworld–State-of-the-art review. Tunn. Undergr. Space Technol. 2007, 22(5–6): 568–586.

Miller, R., 2013. Introduction to this special section: Urban geophysics. Lead. Edge 32 (3), 248–249.

Rodriguez, V., Gutiérrez, F., Green, A.G., Carbonel, D., Horstmeyer, H., Schmelzbach, C., 2014. Characterizing sagging and collapse sinkholes in a mantled karst by means of ground penetrating radar (GPR). Environ. Eng. Geosci. 20 (2), 109–132.

Ronczka, M., Wisen, R., Dahlin, T., 2018. Geophysical pre-investigation for a Stockholm tunnel project: joint inversion and interpretation of geoelectric and seismic refraction data in an urban environment. Near Surf. Geophys. 16 (3), 258–268.

Serzu, M.H., Kozak, E.T., Lodha, G.S., Everitt, R.A., Woodcock, D.R., 2004. Use of borehole radar techniques to characterize fractured granitic bedrock at AECL's Underground Research Laboratory. J. Appl. Geophys. 55 (1–2), 137–150.

Slob, E., Sato, M., Olhoeft, G., 2010. Surface and borehole ground-penetrating-radar developments. Geophysics. 75 (5), 75A103–120.

Spillmann, T., Maurer, H., Willenberg, H., Evans, K.F., Heincke, B., Green, A.G., 2007. Characterization of an unstable rock mass based on borehole logs and diverse borehole radar data. J. Appl. Geophys. 61 (1), 16–38.

Tronicke, J., Hamann, G., 2014. Vertical radar profiling: combined analysis of traveltimes, amplitudes, and reflections. Geophysics. 79, H23–H35.
Wang, J., Yang, T., Wang, Y., 2018. Brief analysis on the history and technical evolution of the construction of Qiantang River seawall. Study Natural Cultural Heritage. 3 (7), 141–145 (in Chinese).
Wang, L., Gu, X., Liu, Z., Wu, W., Wang, D., 2022. Automatic detection of asphalt pavement thickness: a method combining GPR images and improved Canny algorithm. Measurement. 196, 111248.
Wänstedt, S., Carlsten, S., Tirén, S., 2000. Borehole radar measurements aid structure geological interpretations. J. Appl. Geophys. 43 (2–4), 227–237.
Xu, H., 2004. Ancient and modern Qiantang River seawall. Zhejiang Hydrotechnics. 63–65 (in Chinese).
Zhao, W., Forte, E., Pipan, M., Tian, G., 2013. Ground penetrating radar (GPR) attribute analysis for archaeological prospection. J. Appl. Geophys. 97, 107–117.
Zhao, W., Forte, E., Colucci, R.R., Pipan, M., 2016a. High-resolution glacier imaging and characterization by means of GPR attribute analysis. Geophys. J. Int. 206 (2), 1366–1374.
Zhao, W., Forte, E., Pipan, M., 2016b. Texture attribute analysis of GPR data for archaeological prospection. Pure Appl. Geophys. 173 (8), 2737–2751.
Zhao, W., Forte, E., Fontolan, G., Pipan, M., 2018. Advanced GPR imaging of sedimentary features: integrated attribute analysis applied to sand dunes. Geophys. J. Int. 213 (1), 147–156.